A Static Model of Upper Main Sequence Stars

Matthew Siebert
(Dated: December 6, 2016)

Static models of stellar structure were created for a variety of different main sequence stars. Each of these stars had a H, He and metal fraction of 0.7, 0.28, and 0.02 respectively. The model assumed spherical symmetry, hydrostatic equilibrium, and the absence of a magnetic field. It was also assumed that the gas within the star was fully ionized, and that the only contributors to energy generation were nuclear processes. Radius, luminosity, pressure and temperature were all computed as a function of the total mass enclosed within a spherical shell. The numerical method of shooting to a fitting point was used in order to find a solution. Solutions using this model would only converge in the mass range of $1.5 - 30\ M_{\odot}$.

I. INTRODUCTION

When a star is on the main sequence, it will stay there while stably fusing Hydrogen into Helium for several billion years. The energy produced from the reactions in the core causes a thermal pressure that balances the inward pressure from gravitational collapse. By choosing specific stellar properties, we essentially select a specific moment of time on the main sequence. Since the timescale for evolution of stellar structure is very long, we can develop basic static models that describe these main sequence stars. The purpose of this assignment was to numerically solve the four coupled differential equations of stellar structure for stars of our choosing. The equations are as follows:

$$\frac{\partial r}{\partial m} = \frac{1}{4\pi r^2 \rho} \tag{1}$$

$$\frac{\partial l}{\partial m} = \epsilon_n + \epsilon_g - \epsilon_\nu \tag{2}$$

$$\frac{\partial P}{\partial m} = -\frac{Gm}{4\pi r^4} \tag{3}$$

$$\frac{\partial T}{\partial m} = -\frac{GmT}{4\pi r^4 P}\nabla \tag{4}$$

These equations describe how different parameters change with mass. Equation 1 describes the radius r assuming spherical symmetry at a given mass shell, Equation 2 describes the energy generation rate l, Equation 3 describes the total pressure P assuming hydrostatic equilibrium, and Equation 4 describes the temperature T. These equations are all coupled, so we need to integrate them simultaneously in order to obtain their solutions.

II. THEORETICAL BACKGROUND

A. Density and Mean Molecular Weight

The density ρ in Equation 1 is determined by assuming that the total pressure is the sum of the pressure from the ideal gas law and pressure from radiation:

$$P = \frac{\mathbb{R}}{\mu}\rho T + \frac{a}{3}T^4 \tag{5}$$

$$\mu = \frac{2}{1 + 3X + \frac{Y}{2}} \tag{6}$$

where $\mathbb{R} = 8.315{\cdot}10^7\ erg{\cdot}K^{-1}g^{-1}$ and $a = 7.56464{\cdot}10^{-15}\ erg \cdot cm^{-3}K^{-4}$. μ is the mean molecular weight of the gas within the star and is described by Equation 6. X and Y are the mass fractions of Hydrogen and Helium respectively. This equation assumes that the gas is fully ionized at every point in the star.

B. Energy Generation

The primary source of energy in stars is through the fusion of light nuclei. At high pressure and temperature the nuclei have enough energy to approach close enough so that the strong force dominates over Coulomb forces. On the main sequence hydrogen burning dominates the energy generation within the star. The $proton-proton(pp)$ chain and the CNO cycle are the two main series of reactions in the hydrogen burning regime. Therefore in Equation 2, $\epsilon_n = \epsilon_{pp} + \epsilon_{CNO}$. The specific energy generation rates for these reactions can be approximated with the following equations:

$$T_n = \frac{T}{10^n} \tag{7}$$

$$\begin{aligned} \epsilon_{pp} &= 2.57 \cdot 10^4 \psi f_{11} g_{11} X^2 T_9^{-2/3} e^{-3.381/T_9^{1/3}}, \\ g_{11} &= (1 + 3.82T_9 + 1.51T_9^2 + 0.144T_9^3 - 0.0114T_9^4) \end{aligned} \tag{8}$$

$$\begin{aligned} \epsilon_{CNO} &= 8.24 \cdot 10^{25} g_{14,1} X_{CNO} X \rho T_9^{-2/3} e^{-15.231 T_9^{-1/3} - (T_9/0.8)^2}, \\ g_{14,1} &= (1 - 2.00T_9 + 3.41T_9^2 - 2.42T_9^3) \end{aligned} \tag{9}$$

The pp chain energy production depends largely on the initial mass fraction of Helium. This is due to the fact that the pp chain contains three reaction channels. Two of these channels require the presence of ^{4}He. The factor ψ accounts for the extra energy generated for a given Helium mass fraction Y. The dependence of ψ on T for three values of Y(X_{He} in the figure) is shown in Figure

1. The way we determine this parameter for arbitrary values of Y is defined in section III A. The factor f_{11} is

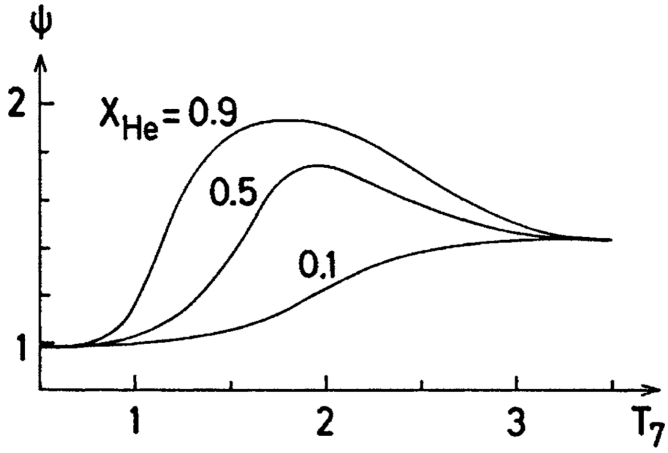

FIG. 1. Correction ψ for three different He abundances [1]

the electron shielding factor. Since particles approaching each other see the net charge of the other nucleus plus the electron cloud, the electron cloud can have a large effect on the reaction rate at high densities. Main sequence stars have weak screening, so this effect is negligible and $f_{11} \sim 1$.

In Equation 9, X_{CNO} is the sum of the mass fractions of Carbon, Oxygen, and Nitrogen. This is typically taken to be $0.7 \cdot Z$ where Z is the mass fraction of all metals. Figure 2 shows the strong dependence of temperature on the dominant burning mechanisms. It is evident that the CNO cycle is dominant at higher temperatures, so we expect more CNO burning for larger stars. We also expect to have a convective core in this burning regime.

Finally, since the star is not evolving on the timescale of our model, we can assume that the energy generation due to gravitational contraction (ϵ_g) is negligible. We can also assume that the energy carried away by neutrinos (ϵ_ν) is negligible when compared to the nuclear energy generation in Equation 2.

C. Temperature Gradient

In Equation 4, $\nabla = \frac{dlnT}{dlnP}$. Its value depends heavily on whether or not the energy transport at a given mass shell in the star is radiative or convective. The radiative and convective ∇ are shown below

$$\nabla_{rad} = \frac{3}{16\pi acG}\frac{\kappa l P}{m T^4} \tag{10}$$

$$\nabla_{ad} = 0.4 \tag{11}$$

where κ is the opacity and c is the speed of light. In a convective region the gas is well mixed and can be approximated as adiabatic (constant temperature gradient). In order to determine ∇, one would need to employ

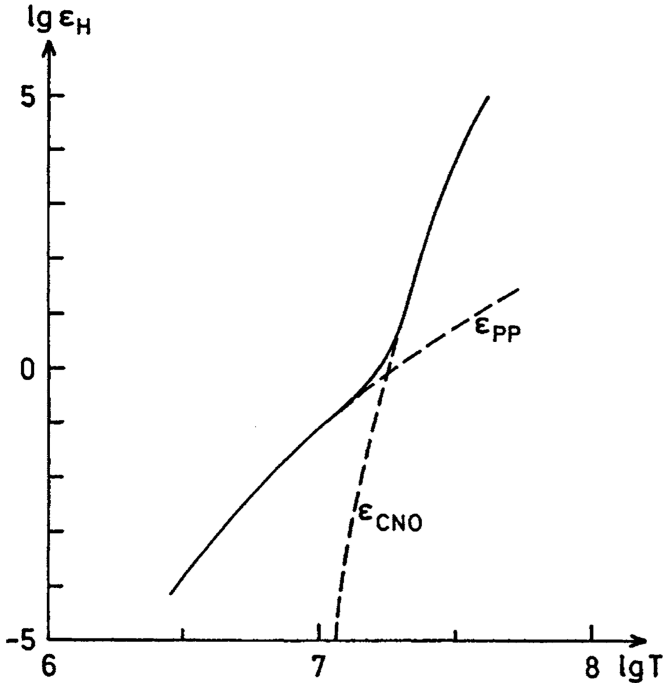

FIG. 2. Contributions to total energy generation from the pp-chain and CNO cycle [1]

"mixing-length" theory because it treats convection locally. ∇ is approximated with the minimum of ∇_{rad} and ∇_{ad}.

The description for finding the opacity at a given point in the star is in section III A.

III. NUMERICAL METHOD

The physical problem presented in section II is a two-point boundary value problem. We specify conditions that we know must be satisfied in the center and on the surface of the star. Then we use a method of integration in order to find a solution that obeys these conditions.

A. Interpolation Methods

A few of the parameters in the equations shown so far require the use of interpolation in order to get accurate values.

We often require the knowledge of the opacity of a gas at a certain point within the star. This model uses type 1 (fixed relative metal distribution) opacity tables generated from The Opal Opacity Code [4] in order to determine the opacity of gas at a given density and temperature. The ASCII file contains 126 tables for varying compositions (X, Y, and Z). The function *read_ opacities* in *opacity.py* takes a given X, Y, and Z, and returns the relevant arrays to be fed into an interpolation function.

The function *RectBivariateSpline* in the *scipy.interpolate* module was used for 2D interpolation. Since the opacity tables are not rectangular, the portions of the tables at high temperatures were removed. The lowest temperature on each of these tables is $logT = 3.75$. This means that the surface of the sun is right at the boundary of these tables. The models for this project are done for hotter stars in order to avoid poor interpolations.

Another parameter that required interpolation was the *pp*-chain correction factor ψ. The only information available about this parameter is presented in Figure 1. Therefore, a series of ten points on each line were chosen and fed into the same interpolation function. This allowed for a decent estimate of ψ for a given Helium mass fraction and temperature.

B. Boundary Conditions

Before we can attempt integration we need to calculate the values of r, l, P, and T at the boundaries. This problem is made difficult by the fact that we cannot define these parameters exactly at the center and the surface of the star.

At the center of the star we can guess P_c and T_c and set $r = l = 0$, but we cannot start the integration directly at the center because $m \to 0$ there. Instead we must define a point near the center and estimate the conditions there.

$$r = \left(\frac{3}{4\pi\rho_c}\right)^{1/3} m^{1/3} \tag{12}$$

$$l = (\epsilon_n + \epsilon_g - \epsilon_\nu)m \tag{13}$$

$$P - P_c = -\frac{3G}{4\pi}\left(\frac{4\pi}{3}\rho_c\right)^{4/3} m^{2/3} \tag{14}$$

$$T^4 - T_c^4 = = -\frac{1}{2ac}\left(\frac{3}{4\pi}\right)^{2/3} \kappa_c \epsilon \rho_c^{4/3} m^{2/3} \tag{15}$$

$$lnT - lnT_c = -\left(\frac{\pi}{6}\right)^{1/3} G\frac{\nabla_{ad,c}\rho_c^{4/3}}{P_c} m^{2/3} \tag{16}$$

Equations 12 - 16 come from expanding r about $m = 0$. These equations can be used to calculate r, l, P, and T at a mass shell slightly outside of the center of the star. Equations 15 and 16 define the initial temperature for a region that is fully radiative or fully convective respectively. The function *load1* in *shoot_ routines.py* calculates these boundary conditions and supplies the initial conditions for the outward integration.

We define the surface of the star to be at the location of the photosphere. This is found to be where the optical depth τ is equal to 2/3. Since the bulk of the radiation is emitted into space at this location, the total luminosity and effective temperature can be used as boundary conditions. Therefore the surface conditions are as follows:

$$r = R \tag{17}$$

$$l = L \tag{18}$$

$$P = \frac{GM}{R^2}\frac{2}{3}\frac{1}{\bar{\kappa}} \tag{19}$$

$$T = \left(\frac{L}{4\pi R^2 \sigma}\right)^{1/4} \tag{20}$$

The pressure surface condition (Equation 19) comes from requiring hydrostatic equilibrium at the location in the star where $\tau = 2/3$. This condition takes some care because we must ensure that Equation 19 is also consistent with the ideal gas law. First, a range of densities was defined by the available range in the opacity interpolation table. Then, a corresponding range of pressures was calculated for a given T (from Equation 20). κ was then determined through the interpolation method described in Section III C at each of these pressures. While iterating, the pressure calculated from Equation 19 was compared to the pressure determined through the ideal gas law (plus radiation pressure). The pressure that minimized this difference was chosen as the surface pressure. The function *load2* in *shoot_ routines.py* calculates these boundary conditions and supplies the initial conditions for the inward integration.

C. Parameters

The parameters used for these models are shown in Appendix A, Table I. At the center we guess the pressure and temperature (P_c and T_c), and at the surface we guess the radius and total luminosity (R and L). These values were obtained from the results of polytropic models from section 2.15 of Hansen, Kawaler and Trimble [3]. If the boundary conditions are far off from the properties of a real star, then the solutions may not match well at the fitting point and the iterative method may never converge.

D. Shooting to a Fitting Point

After determining the boundary conditions, the equations of stellar structure could be integrated to determine a solution for r, l, P, and T as a function of mass. Since the solutions depend largely on the chosen initial conditions, simply integrating from one side to the other will never satisfy all of the boundary conditions. For this reason we use the method of shooting to a fitting point. The equations are integrated starting from the center and starting from the surface to a fitting point ($M_{tot}/2$ in this case). The initial conditions are then changed iteratively until the difference between the outward and inward solutions is minimized. The function *odeint* from the Python module *scipy.integrate* was use to perform both the outward and inward integrations.

After the initial integrations, the differences (for r, l, P, and T) between the solutions are stored in an array. This is called the discrepancy vector $\mathbf{F}$. The four free boundary conditions are R and L at the surface, and P_c, and T_c at the center. During the first iteration, a small 1% correction is made to each parameter ($\delta\mathbf{V} = 0.01 \cdot [R, L, P_c, T_c]$). The integration for each of these corrections is done independently in order to populate the Jacobian matrix in Equation 24. The derivatives in the equations are calculated through the finite difference method.

$$\mathbf{F} = [R_{diff}, L_{diff}, P_{Diff}, T_{diff}] \tag{21}$$

$$\delta\mathbf{V} = [\delta R, \delta L, \delta P, \delta T] \tag{22}$$

$$\mathbf{J} \cdot \delta\mathbf{V} = -\mathbf{F} \tag{23}$$

$$J_{ij} = \frac{\partial F_i}{\partial V_j} \tag{24}$$

The goal of this iterative process is to zero the discrepancy matrix. This is accomplished by solving the matrix equation for $\delta\mathbf{V}$ (Equation 23). This was done using the *linalg* module from Python's *numpy*. A fraction (in this case 20%) of the $\delta\mathbf{V}$ that is calculated is applied in the next iteration. This process is continued until the discrepancy matrix is minimized to some tolerance. The tolerance for this model was $10^{-4} \cdot [R, L, P_c, T_c]$. The function *shoot_and_fit* in *shoot.py* controls this iterative solution. Each iteration required ten integrations total, and the solution converged after about 30 - 40 iterations.

IV. RESULTS

Figures 3 - 6 show the converged solution for a two solar mass star with the initial parameters described in Appendix A, Table I. The blue and green lines correspond to the outward and inward solution respectively.

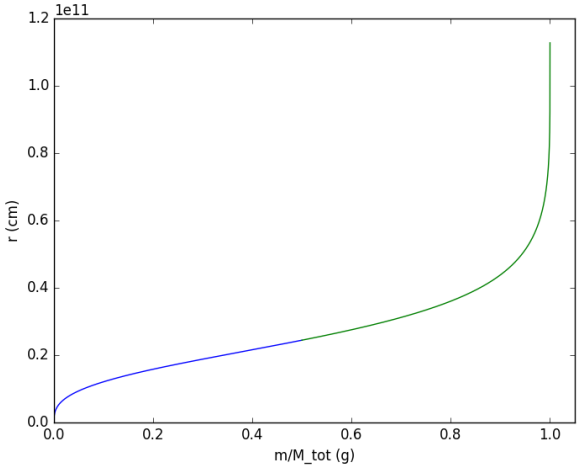

FIG. 3. Radius vs. Fraction of Total Mass, $M_{tot} = 2M_\odot$

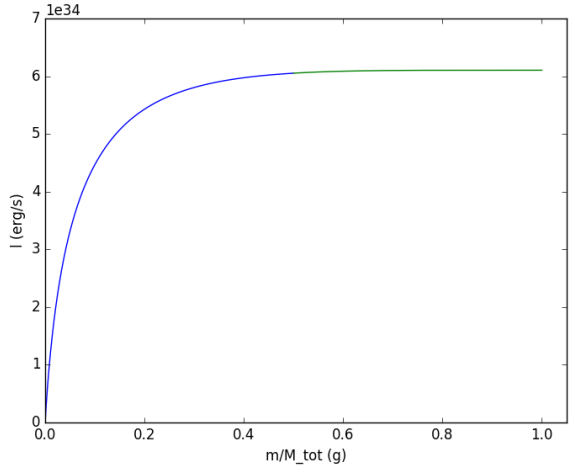

FIG. 4. Luminosity vs. Fraction of Total Mass, $M_{tot} = 2M_\odot$

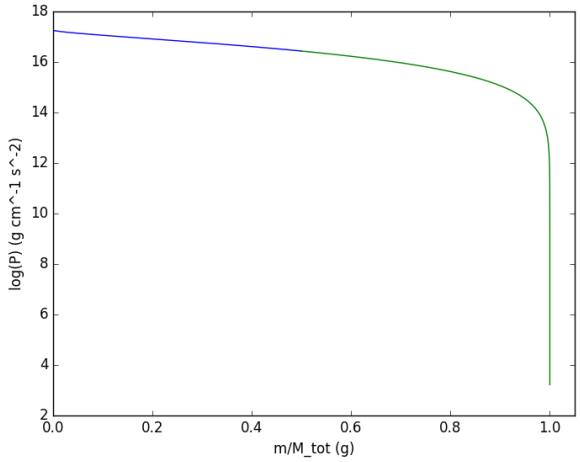

FIG. 5. Pressure vs. Fraction of Total Mass, $M_{tot} = 2M_\odot$

All of these plots show a smooth transition at the fitting point. It is evident that the temperature and pressure rapidly drop off near the surface. This meant that a much smaller step size was needed in order to correctly perform the inward integration.

Table II in Appendix A shows the boundary conditions of the converged solution. For the two solar mass star, these correspond to a 9.70%, -12.8%, 11.7%, and 0.474% differences from the initial guesses of R, L, P_c, and T_c respectively. The other models produce similar relationships to those represented in Figures 3 - 6. Through comparison of Table I to Table II in Appendix A, we can determine the accuracy of our initial guesses for each star.

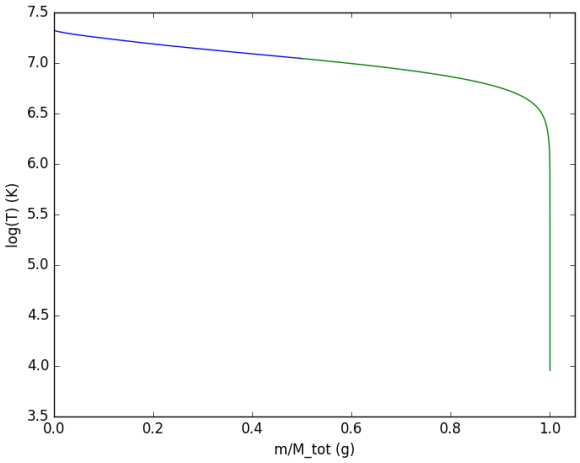

FIG. 6. Temperature vs. Fraction of Total Mass, $M_{tot} = 2M_{\odot}$

V. DISCUSSION

The results of these models seem to be in rough agreement with the parameters found in the polytropic models [3]. Since the model converged for a relatively large numbers of stars, a Hertzsprung-Russell diagram could be created (Figure 7). Since the initial parameter guesses

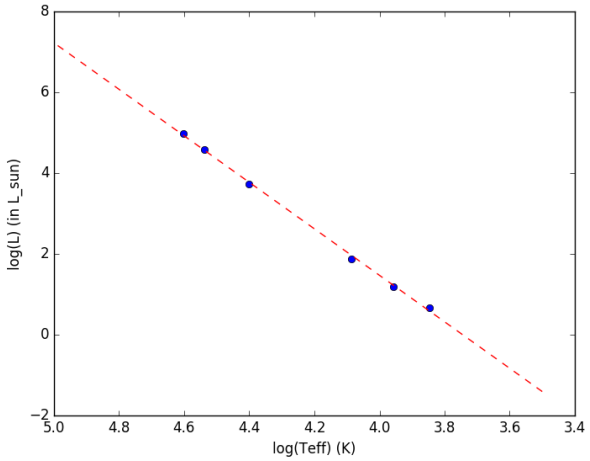

FIG. 7. H-R Diagram using model results from Table II (Appendix A)

only tended to be off by $\sim 10\%$ it is not surprising that the model converges quickly and we obtain an H-R diagram that is consistent with observations. The stars clearly form a main sequence line. The slope of this diagram yielded a Temperature-Luminosity relationship of $L \, \alpha \, T^{5.75}$. The corresponding Mass-Luminosity relationship is $L \, \alpha \, M^{3.34}$ which is in agreement with the results in Chapter 20 of Kippenhahn [1].

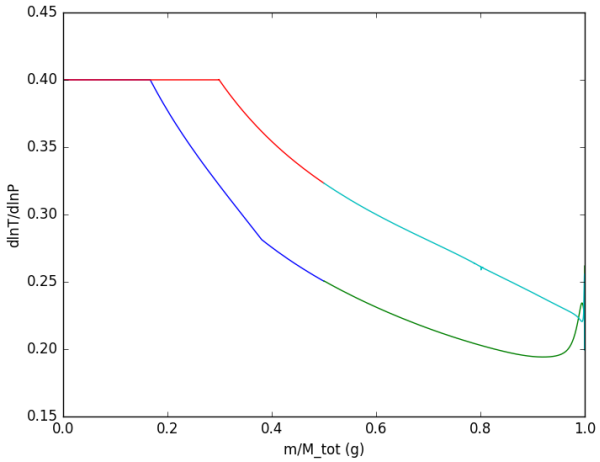

FIG. 8. Temperature gradient (∇) vs. Fraction of Total Mass. Blue and green lines are outward and inward solutions respectively for a $2M_{\odot}$ star. Red and teal lines are outward and inward solutions respectively for a $20M_{\odot}$ star.

One of the most important results is shown in Figure 8. We can directly see the effect that a stars mass has on its interior structure. Chapter 22.3 of Kippenhahn [1] states that there are two main types of models for stars on the main sequence. Upper main sequence stars have a convective core and a radiative envelope, while lower main sequence stars have a radiative core and convective envelope. The transition from one model to the other occurs at about $1M_{\odot}$. Therefore, we expect that all of the stars in our model should be the former model.

As evidenced by the plateaus at $\nabla = 0.4$, both the 2 and $20M_{\odot}$ stars have convective cores. We also see that the convective region in the lower mass star constitutes a smaller fraction of the total mass of the star. The central temperature of the 2 and $20M_{\odot}$ stars were determined to be $2.12 \cdot 10^7$ K and $3.63 \cdot 10^7$ K respectively. As shown in section II B, the energy generated by the CNO cycle increases rapidly with temperature. Therefore convective energy transport is is extremely efficient farther out in larger mass stars on the upper main sequence.

VI. CONCLUSION

Static stellar models were developed for stars in the range of $1.5 - 30 \; M_{\odot}$. We were able to show how radius, luminosity, pressure and temperature change with the mass enclosed throughout the star. We assumed spherical symmetry, hydrostatic equilibrium, no magnetic field, fully ionized gas, and energy generation from nuclear reactions only. This model would not converge for stellar masses outside of the range described above.

The boundary conditions near the center were determined by expanding r about $m = 0$ and then calculating the corresponding l, P and T given the central pressure and temperature (guessed). The surface was defined as the radius at which the optical depth $\tau = 2/3$. R and L are guessed at the surface. P was determined with the given τ and the condition for hydrostatic equilibrium. It was then checked to be consistent with the ideal gas law. T at the surface was determined the Stefan-Boltzmann law.

The method of shooting to a fitting point was used in order obtain a solution that satisfied all of the boundary conditions. Generally, this iterative method made small changes to the initial conditions in order to fit a solution from the inward integration to the solution from the outward integration at a specific point in the star. The model tended to converge after about $30 - 40$ iterations.

Figures 3 - 6 show the converged solution for a $2M_{\odot}$ star. The structures of the other stars produced by this model had the same relative shapes but approached their appropriate boundary conditions shown in Table II. This model shows that the rapid fall off of pressure and temperature near the surface of the star occur within a very thin mass shell.

An H-R diagram was also produced (Figure 7) with the six stars modeled in this paper. The converged total luminosity and effective temperature seem to be in agreement with observations of upper main sequence stars. We recover a mass-luminosity relationship of $L \ \alpha \ M^{3.34}$.

Finally, these upper main sequence stars showed evidence for a convective core and radiative envelope (Figure 8). The larger mass stars have convective envelopes that extend farther out. This is consistent with our understanding of how energy generation from the CNO cycle varies with temperature.

There are a number of improvements that could be made in order to improve this basic model. For example, we could obtain larger opacity tables in order to model the structure of lower main sequence stars with lower temperatures. We could also implement a better estimation of the ionization state of the gas within the star. Also, the implementation of mixing length theory could provide a better estimate of the temperature gradient throughout the star especially near the transition from a convective core to a radiative envelope.

VII. USING THE MODEL

The scripts necessary for running this model are *shoot.py, shoot_routines.py, density_model.py, opacity.py* and *constants.py*. The file *opacity_tables.txt* is also required. The script *shoot.py* is the main controller code used to find and plot a solution for a specific star. Once initial guesses are defined and mass ranges are set, the program calls the function *shoot_and_fit*. This function implements the numerical procedure described in section III D.

The script *shoot_routines.py* defines five useful functions that are used within the main controller script. *load1* and *load2* calculate and return the boundary conditions at the center and the surface of the star respectively. The function *ep_correction* creates and returns an interpolation table that is used to find the correction factor ψ to the $pp - chain$ energy generation. The function *ep_n* calculates the total specific nuclear energy generation and a temperature T. Finally, the function *derivs* returns the derivatives (Equations 1 - 4) at a point in the star with enclosed mass m.

The script *density_model.py* defines a few functions for determining mean molecular weight, density, and total pressure using some given parameters.

The script *opacity.py* defines a function *read_opacities* which takes a given composition (X, Y, and Z), searches the file *opacity_tables.txt* for the corresponding opacity table, and returns arrays containing the relevant information for interpolation within in this table.

The script *constants.py* contains some of the relevant constants that are used often in this model.

[1] R. Kippenhahn, A. Weigert, A. Weiss. *Stellar Structure and Evolution. Second Edition.* Springer. 2012.

[2] W. H. Press, S. A, Teukolsky, W. T. Vetterling and B. P. Flannery *Numerical Recipes, The Art of Scientific Computing, 3rd edit.,*. Camb. Univ. Press 2007.

[3] C. Hansen, S. Kawaler, V. Trimble. *Stellar Interiors: Physical Principles, Structure, and Evolution. Second Edition* Springer. 2004.

[4] *"Opal Opacity Tables"* C. Iglesias. 1999. http://opalopacity.llnl.gov/existing.html

VIII. APPENDIX A

$M_{tot}(M_\odot)$	1.5	2	3	10	20	30
$R(cm)$	$9.15 \cdot 10^{10}$	$1.03 \cdot 10^{11}$	$1.28 \cdot 10^{11}$	$2.59 \cdot 10^{11}$	$3.87 \cdot 10^{11}$	$4.85 \cdot 10^{11}$
$L(erg \cdot s^{-1})$	$2.20 \cdot 10^{34}$	$7.00 \cdot 10^{34}$	$3.42 \cdot 10^{35}$	$2.26 \cdot 10^{37}$	$1.64 \cdot 10^{38}$	$4.46 \cdot 10^{38}$
$P_c(g \cdot cm^{-1} \cdot s^{-2})$	$1.91 \cdot 10^{17}$	$1.62 \cdot 10^{17}$	$1.15 \cdot 10^{17}$	$3.72 \cdot 10^{16}$	$2.34 \cdot 10^{16}$	$1.95 \cdot 10^{16}$
$T_c(K)$	$1.91 \cdot 10^{7}$	$2.11 \cdot 10^{7}$	$2.35 \cdot 10^{7}$	$3.05 \cdot 10^{7}$	$3.43 \cdot 10^{7}$	$3.63 \cdot 10^{7}$
X	0.7	0.7	0.7	0.7	0.7	0.7
Y	0.28	0.28	0.28	0.28	0.28	0.28
Z	0.02	0.02	0.02	0.02	0.02	0.02
X_{CNO}	$0.7 * Z$	$0.7 * Z$	$0.7 * Z$	$0.7 * Z$	$0.7 * Z$	$0.7 * Z$

TABLE I. Chemical composition and initial guesses for boundary conditions

$M_{tot}(M_\odot)$	1.5	2	3	10	20	30
$R(cm)$	$1.03 \cdot 10^{11}$	$1.13 \cdot 10^{11}$	$1.38 \cdot 10^{11}$	$2.69 \cdot 10^{11}$	$3.82 \cdot 10^{11}$	$4.55 \cdot 10^{11}$
$L(erg \cdot s^{-1})$	$1.84 \cdot 10^{34}$	$6.10 \cdot 10^{34}$	$2.98 \cdot 10^{35}$	$2.06 \cdot 10^{37}$	$1.46 \cdot 10^{38}$	$3.79 \cdot 10^{38}$
$P_c(g \cdot cm^{-1} \cdot s^{-2})$	$1.96 \cdot 10^{17}$	$1.81 \cdot 10^{17}$	$1.27 \cdot 10^{17}$	$3.79 \cdot 10^{16}$	$2.21 \cdot 10^{16}$	$1.77 \cdot 10^{16}$
$T_c(K)$	$1.83 \cdot 10^{7}$	$2.12 \cdot 10^{7}$	$2.41 \cdot 10^{7}$	$3.20 \cdot 10^{7}$	$3.63 \cdot 10^{7}$	$3.85 \cdot 10^{7}$

TABLE II. Converged boundary conditions